Migliorini *et al.*
Journal of Orthopaedic Surgery and Research (2024) 19:411
https://doi.org/10.1186/s13018-024-04918-2

Journal of Orthopaedic Surgery and Research

RESEARCH ARTICLE

Open Access

Osteointegration of functionalised high-performance oxide ceramics: imaging from micro-computed tomography

Filippo Migliorini[1,2,3*†], Jörg Eschweiler[1†], Marcel Betsch[4], Nicola Maffulli[5,6,7*], Markus Tingart[8], Frank Hildebrand[1], Sophie Lecouturier[1], Björn Rath[9] and Hanno Schenker[1]

Abstract

Background This study evaluated the osseointegration potential of functionalised high-performance oxide ceramics (HPOC) in isolation or coated with BMP-2 or RGD peptides in 36 New Zeeland female rabbits using micro-computed tomography (micro CT). The primary outcomes of interest were to assess the amount of ossification evaluating the improvement in the bone volume/ total volume (BV/TV) ratio and trabecular thickness at 6 and 12 weeks. The second outcome of interest was to investigate possible differences in osteointegration between the functionalised silanised HPOC in isolation or coated with Bone Morphogenetic Protein 2 (BMP-2) or RGD peptides.

Methods 36 adult female New Zealand white rabbits with a minimum weight of three kg were used. One-third of HPOCs were functionalised with silicon suboxide (SiOx), a third with BMP-2 (sHPOC-BMP2), and another third with RGD (sHPOC-RGD). All samples were scanned with a high-resolution micro CT (U-CTHR, MILabs B.V., Houten, The Netherlands) with a reconstructed voxel resolution of 10 µm. MicroCT scans were reconstructed in three planes and processed using Imalytics Preclinical version 2.1 (Gremse-IT GmbH, Aachen, Germany) software. The total volume (TV), bone volume (BV) and ratio BV/TV were calculated within the coating area.

Results BV/TV increased significantly from 6 to 12 weeks in all HPOCs: silanised ($P=0.01$), BMP-2 ($P<0.0001$), and RGD ($P<0.0001$) groups. At 12 weeks, the BMP-2 groups demonstrated greater ossification in the RGD ($P<0.0001$) and silanised ($P=0.008$) groups. Trabecular thickness increased significantly from 6 to 12 weeks ($P<0.0001$). At 12 weeks, BMP-2 promoted greater trabecular thickness compared to the silanised group ($P=0.07$), although no difference was found with the RGD ($P=0.1$) group.

Conclusion Sinalised HPOC in isolation or functionalised with BMP-2 or RGD promotes in vivo osteointegration. The sinalised HOPC functionalised with BMP-2 demonstrated the greatest osseointegration.

Keywords Ossification, Implants, Osteointegration, Micro-CT

†Filippo Migliorini and Jörg Eschweiler these authors contributed equally to the final version of the manuscript and shared the first author.

*Correspondence:
Filippo Migliorini
migliorini.md@gmail.com
Nicola Maffulli
n.maffulli@qmul.ac.uk
Full list of author information is available at the end of the article

Introduction

The number of joint arthroplasties is increasing and the debate over implant fixation and bearing surfaces is still ongoing [1, 2]. Also, the number of revision arthroplasties has increased. Component wear and tear and aseptic loosening are two major causes of revision [1, 3]. Aseptic loosening is the cause of revision arthroplasty in approximately 10% of patients in the US [4]. The persistent mechanical load can lead to implant wear and generate micro- and nanoparticles, which can cause an inflammatory reaction resulting in bone resorption**.** Different materials have been manufactured to minimize component wear and tear and implant loosening. Ceramics implants are associated with a low incidence of biologically active particle generation and osteolysis. However, the low fracture toughness and linear elastic behaviour of ceramic implants make them prone to breakage under stress. To overcome these limitations, high-performance oxide ceramics (HPOC) have been introduced [5, 6]. HPOC implants show lower wear and biological response to debris [7]. Nevertheless, as HPOCs are biologically inert, implant osseointegration may be impaired [8, 9]. To overcome this limitation to clinical application, we developed biologically functionalised HPOC [10, 11]. Three different coating modalities were evaluated: (1) isolated silanised HPOC (sHPOC) with or without (2) Arg-Gly-Asp (sHPOC-RGD) or (3) bone morphogenic protein-2 (sHPOC-BMP2) peptide coatings [12–14]. For each coating method, we evaluated contact guidance, adhesions, surrounding mesenchymal stromal cells osteogenic differentiation, and their cytotoxic potential [15, 16]. Moreover, the osseointegration potential of functionalised HPOC was compared with titanium implants in rabbits using histomorphometry [12–14]. All coating modalities similarly promoted in vivo ossification to the titanium implants [12–14].

This study evaluated the osseointegration potential of functionalised sHPOC in isolation or coated with BMP-2 or RGD peptides in 36 New Zeeland female rabbits using micro-computed tomography (micro-CT). The primary outcomes of interest were to assess the amount of ossification evaluating the improvement in the bone volume/ total volume (BV/TV) ratio and the trabecular thickness at 6 and 12 weeks. The second outcome of interest was to investigate possible differences in osteointegration between the functionalised sHPOC in isolation or coated with BMP-2 or RGD peptides. It was hypothesised that functionalised sHPOC coated with BMP-2 or RGD peptides promotes greater osseointegration.

Methods

Sample preparation

The HPOCs used in all experiments were manufactured at the Department of Materials Science and Biomaterial Research of the RWTH University Aachen, Germany, as reported in greater detail previously [15, 17–23]. Briefly, plasma-enhanced chemical vapour deposition (PE-CVD) was used to pair stable organosilane monolayers on the monolithic Al_2O_3 HPOC-based cylinders. HPOC cylinders were functionalised with silicon suboxide (SiOx), which was deposited on the polished cylinders. HPOC were air-dried, cured at 80° for 45 min, and stored in liquid nitrogen until use. One day before the experiments, one-third of the sHPOCs were coated with BMP-2 (sHPOC-BMP2), and another third with RGD (sHPOC-RGD) [12, 13, 15, 18].

Surgical procedure

This study was conducted according to the Animal Welfare Act of the Federal Republic of Germany. This study was approved by the Federal Office for Nature, Environment and Consumer Protection of North Rhine-Westphalia, Federal Republic of Germany (Approval ID: 84–02.04.2016.A434). The investigation involved 36 adult female New Zealand white rabbits with a minimum weight of three kg. Rabbits were randomly divided into three groups (Fig. 1): sHPOCs, sHPOC-BMP2, and sHPOC-RGD.

Before surgery, general anaesthesia was provided with 0,1 ml/mg/kg bodyweight Medetomidin hydrochloride (Domitor, Vetoquinol GmbH, Ismaning, Germany) combined with 0.2 ml Ketamin hydrochloride 10% (Narketan, Vetoquinol GmbH, Ismaning, Germany) via subcutaneous injection. The surgical site was shaved, disinfected with iodine and ethanol, and draped in a sterile fashion. Before incision, 10 mg/kg body weight of Enrofloxacin (Baytril, Bayer Austria GmbH, Wien, Austria) was injected subcutaneously. A longitudinal skin incision was performed over the right lateral femoral condyle. After accurate dissection through the fascia and muscles, the condyle was exposed. The lateral collateral ligament (LCL) was identified as a landmark. Sparing the LCL, a mono-cortical drill hole with a 5.5 mm trephine was prepared, and the HPOC cylinder was inserted in a press-fit fashion. Attention was given not to damage the knee capsule. After irrigation with saline solution, tissues were closed in layers. Finally, the skin was stapled and sealed with a chelated silver spray. For the first three days after surgery, 4 mg/kg bodyweight Carprofen (Rimadyl, Zoetis Deutschland GmbH, Berlin, Germany) was applied every 24 h. At six and 12 weeks postoperatively, the animals were euthanised with 2 ml/kg bodyweight

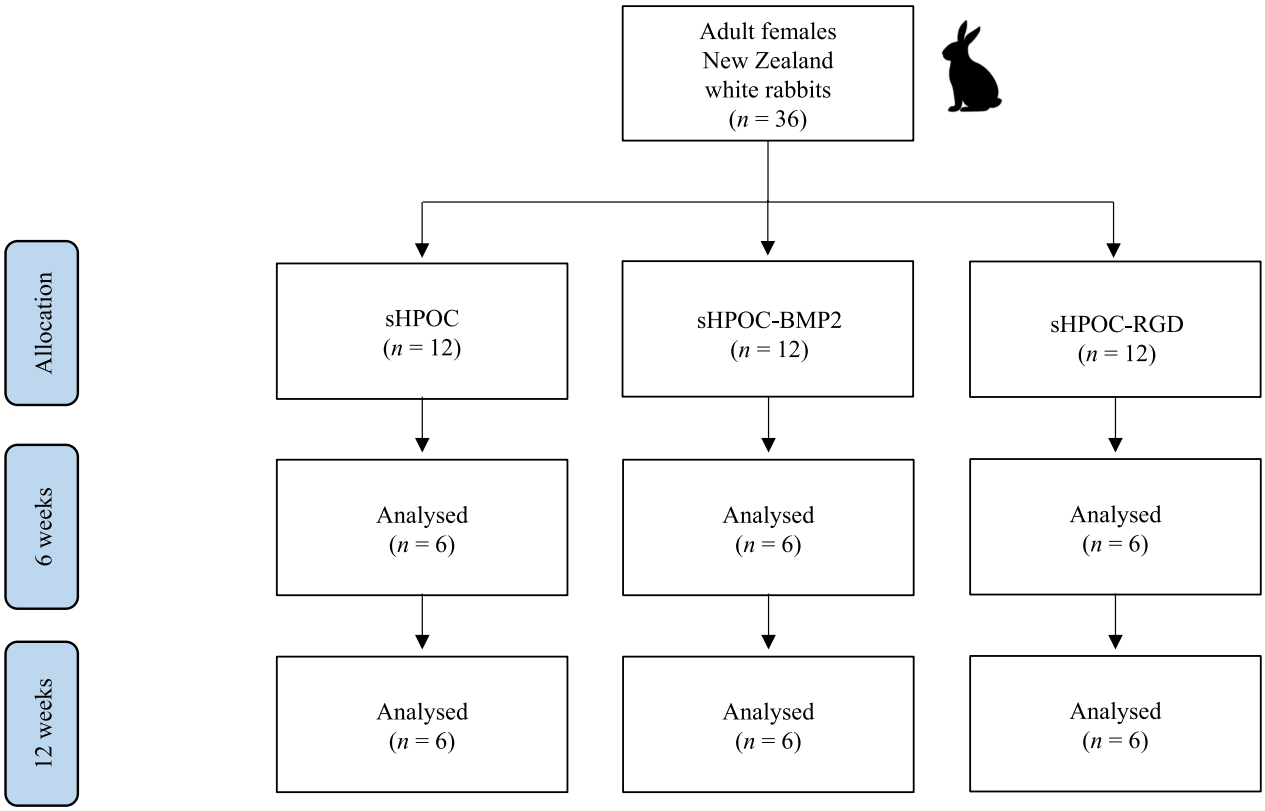

Fig. 1 Study set up

natrium Pentobarbital (Fagron GmbH & Co. KG, Glinde, Germany), and the femoral condyles were harvested en bloc. Fixation was performed over 12 days with 4% paraformaldehyde followed by an alcohol series with ethanol of 50% to 100% and xylol. The specimens were embedded in Technovit® 9100 (Heraeus Kulzer GmbH, Hanau, Germany).

MicroCT evaluation

After PMMA embedding, all samples were scanned with a high-resolution micro CT (U-CT^{HR}, MILabs B.V., Houten, The Netherlands) with a reconstructed voxel resolution of 10 µm. MicroCT scans were reconstructed in three planes and processed using Imalytics Preclinical version 2.1 (Gremse-IT GmbH, Aachen, Germany) software (Fig. 2).

To eliminate any surrounding soft tissue and epoxy a primary density thresholding with a predefined value of 5000 was performed. To gain smoother edges an anti-aliasing was performed manually with 3 voxels. Subsequently, an ROI (coating area) was defined with a value of 10 (Fig. 2). To differentiate between bone and soft tissue another density thresholding with a predefined value of 3000 within the ROI was performed. The bony tissues were marked in white, whereas the surrounding space within the ROI was marked purple. For better visualization and further calculation, a three-dimensional model was calculated (Fig. 3).

To eliminate the bias caused by the bony approach on the lateral aspect of the implant within the ROI, a predefined crop was performed in all samples (Fig. 4). The cropped region was not considered for further calculation. After performing the cropping, a three-dimensional model was calculated for better visualization and following measures (Fig. 5).

The total volume (TV) of the ROI was determined. Within the TV, the bone volume (BV) was evaluated, and the ratio BV/TV was calculated using an implemented feature of the Imalytics software. Finally, the trabecular thickness was measured using an implemented tool of the Imalytics software. Data were extracted to Microsoft Office Excel version 2016 (Microsoft Corporation, Redmond, Washington, USA).

Outcomes of interests

The outcomes of interest were to evaluate the BV/TV ratio and the trabecular thickness (µm) of each group and compare them at 6 and 12 weeks of follow-up.

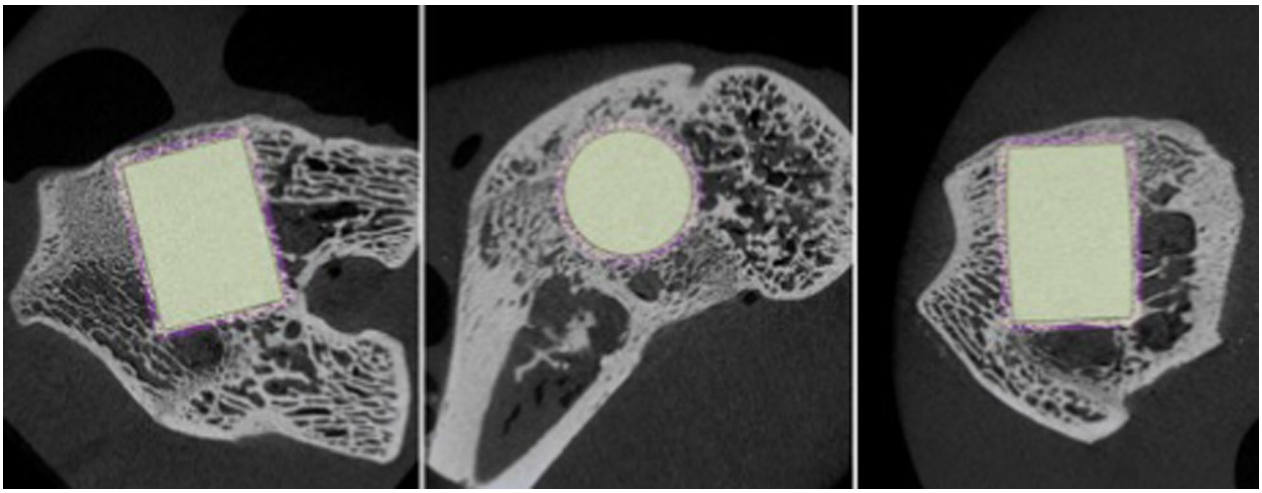

Fig. 2 Three-dimensional MicroCT sequences of the condyle and implants. The interface bone implant (region of interest, ROI) is highlighted around the implant

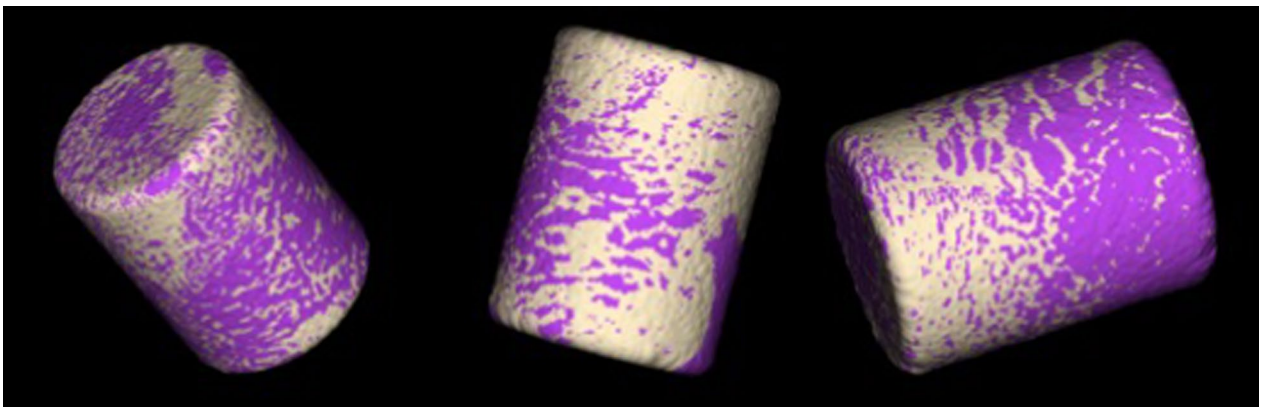

Fig. 3 Three-dimensional Surface Implant after thresholding (White = Bony tissue)

Statistical analysis

The statistical analyses were conducted by one author (**) using the software STATA / MP, version 14.1 (Stata Corporation, College Station, Texas, USA). To investigate whether the within-group BV/TV ratio and the trabecular thickness improved between 6 and 12 weeks, the mean difference (MD) effect measure and standard error (SE) were used. The paired two-tailed t-test was performed.

To compare the between-group BV/TV ratio and the trabecular thickness at 6- and 12 weeks, analysis of variance (ANOVA) was used. The variance (VAR), the sum of squares (SS), and the Fisher-Snedecor distribution (F) were analysed. If $P_{ANOVA} < 0.05$, the Tukey Honestly Significant Difference (HSD) posthoc test was performed to investigate each direct comparison. Confidence intervals were set at 95%. Values of $P < 0.05$ were considered statistically significant.

Results

Animal characteristics

34 rabbits survived the 6- or 12-week experimental period. One rabbit in the RGD group and one in the BMP-2 group perished. Five wounds dehiscence were stapled. At euthanasia, no clinical signs of inflammation or adverse tissue reactions were observed. All implants remained in situ. The mean weight of the rabbits increased from baseline to the last follow-up of + 501.3 mg.

Evaluation of BV/TV ratio

Within-group BV/TV ratio increased significantly from 6 to 12 weeks in all experiments (Table 1): isolated silanised HPOC (MD 2.21; $P = 0.01$), silanised HPOC coated BMP-2 (MD 5.53; $P < 0.0001$), and coated RGD (MD 1.03; $P < 0.0001$). The ANOVA test showed no between-group difference at 6 ($P = 0.06$) and 12 weeks ($P = 0.1$).

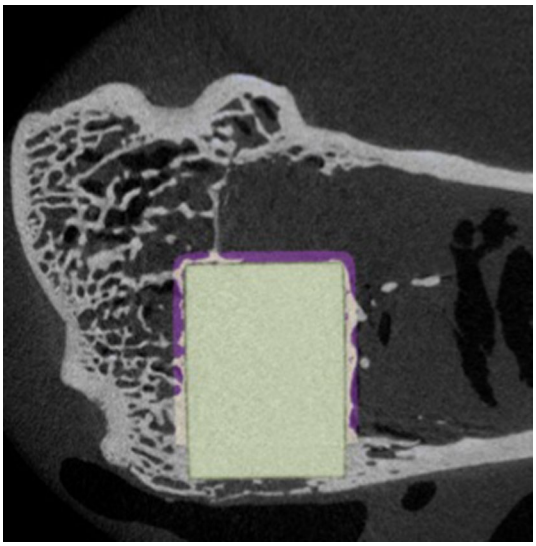

Fig. 4 Two-dimensional MicroCT sequence showing the cropped area (lateral deleted ROI) and showing the surgical defect area on the lateral aspect of the implant

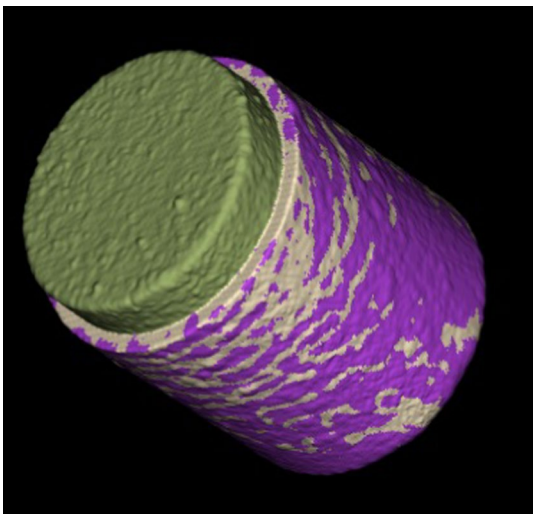

Fig. 5 Three-dimensional model showing the cropped area, bony tissue in white and soft tissue in purple

Evaluation of trabecular thickness

Within-group trabecular thickness (μm) increased significantly from 6 to 12 weeks in all experiments (Table 2): silanised HPOC (MD 1.92; P < 0.0001), silanised HPOC coated BMP-2 (MD 2.20; P < 0.0001), and coated RGD (MD 3.15; P < 0.0001). The ANOVA test showed no between-group difference at 6 (P = 0.1) and 12 weeks (P = 0.1).

Discussion

According to the main findings of the present study, silanised HOPCs in isolation or functionalised with BMP-2 or RDG peptide promoted similar osteointegration in vivo. BV/TV ratio and trabecular thickness increased significantly from 6 to 12 weeks in all HPOCs. However, we were unable to demonstrate a statistically significant difference between the three groups.

Although ceramic is bioinert, its material topography, such as roughness and surface structure, influences cellular response [24, 25]. The microcapillary array structures on the alumina ceramics promoted mesenchymal cell migration, and bone mineralisation [16]. Over the past years, many inorganic materials have been employed to overcome the problem of ceramic bio inertia such as hydroxyapatite and bioactive glasses [26, 27]. Böke et al. [15] showed an increment of cell adhesion using an interfacial layer of silicon suboxide. PE-CVD enhanced the interfacial bond strength between the ceramic and silicon layer and produced high-degree cross-linking within the film [15]. Our previous study investigated the differences in osseointegration between HPOCs and titanium implants. A greater osteoid implant contact in the HPOCs group than in the titanium group after 6 weeks was evident [14]. The silica layer promotes protein absorption that facilitates cell attachment on the implant's surface [28].

BMP-2 promotes osteoblast proliferation, stimulates mineralisation, and enhances mRNA and protein expression of the main osteogenic inductors [29]. BMP-2-enhanced scaffolds have been employed to treat bone defects, inducing significant bone regeneration [30, 31]. High BMP-2 concentration can activate the osteolytic pathway [32]. Hunziker et al. [33] conducted an animal study on 18 sheep comparing titanium implants coated with different concentrations of BMP-2 versus control non-coated implants. After 3 weeks the implants with the highest dose of BMP-2 showed a bone-implant contact ratio (BIC) decrement compared to the control group.

Table 1 BV/TV at 6 and 12 weeks (MD: mean difference; SE: standard error; CI: confidence interval)

Endpoint	6 weeks	12 weeks	MD	SE	95% CI	*P*
Silanised	8.7 ± 2.0	10.9 ± 3.1	2.2	0.821	3.87 to 0.54	0.01
BMP-2	4.7 ± 1.2	10.2 ± 2.4	5.5	0.598	6.74 to 4.31	< 0.0001
RGD	6.3 ± 1.6	9.7 ± 2.1	3.4	0.579	4.57 to 2.22	< 0.0001

Table 2 Trabecular thickness (μm) at 6 and 12 weeks (MD: mean difference; SE: standard error; CI: confidence interval)

Endpoint	6 weeks	12 weeks	MD	SE	95% CI	*P*
Silanised	5.67 ± 0.46	7.59 ± 1.04	1.92	0.251	1.40 to 2.43	< 0.0001
BMP-2	5.55 ± 0.77	8.00 ± 1.20	2.45	0.319	1.80 to 3.09	< 0.0001
RGD	5.55 ± 0.47	8.70 ± 1.00	3.15	0.247	2.64 to 3.65	< 0.0001

The rest of the BMP-2 implants showed an increment in BIC compared to the control group. We previously compared the osseointegration of HPOCs functionalised with BMP-2 implants and titanium implants in 36 rabbits [12]. BIC was higher in the BMP-2 group than in the control group after 6 and 12 weeks. Osteoid implant contact was higher in the BMP-2 group than in the control group after 6 weeks, with no statistically significant difference after 12 weeks.

RGD peptide mediates integrin-specific cell adhesion [34]. RGD-integrin complex binds mesenchymal cells and activates intracellular signalling by different kinds of pathways that lead to the activation of RUNX2 and osteocalcin [34, 35]. It promotes mesenchymal cell migration, osteoblast differentiation and osseointegration [36]. Rappe et al. [37] compared RGD-coated titanium implants, thermally bioactivated titanium implants and titanium implants in 18 rabbits. No statistically significant difference in BIC was found between the three groups after 4 and 12 weeks. Quantitatively comparing the three groups, RGD implants showed the highest BIC. In our previous study on 36 rabbits, the differences between HPOCs functionalised with RGD implants and titanium implants were analysed [12]. The RGD group showed higher BIC than the titanium group after 6 and 12 weeks. No statistically significant difference existed between the two groups after 12 weeks.

The stability of a prosthetic implant is crucial to avoid aseptic loosening and implant failure [38, 39]. Final implant stability is reached in two steps [40]. Primary stability depends on the relative micromovement between the bone and the implant induced by the physiological joint loading [41]. Implant positioning, surgical technique, and bone quality can influence primary stability [42]. Secondary stability is given by the osseointegration process [43]. Osseointegration guarantees the proper anchorage of the implant to the bony tissue [44]. The first radiographic signs of osseointegration are visible three months after surgery [45]. The process of osseointegration of HPCO implants is faster than titanium implants [12, 14]. A meta-analysis on 21,000 total knee arthroplasties demonstrated a statistically significant association between early migration of tibial components and late revision for aseptic loosening [46]. Strait et al. [47] investigated the early mobilisation of the implant in 158 cementless THA. Early mobilisation, up to two years postoperatively was a risk factor for aseptic loosening. The faster secondary stability is reached, the lower the rate of early mobilisation of the implant. BMP-2 implants showed the highest osseointegration potential after 12 weeks [47], but longer follow-up studies are needed.

Our results confirm that biological augmentation of ceramic implants promotes osseointegration. At present, few studies analyse the in vivo interactions between bone tissue and HPOC implants, and our results must be confirmed by further studies on a larger population with longer follow-up.

This study has some limitations. Firstly, animal models do not fully translate to human models. Differences exist in biological processes, functional anatomy, and mechanical loads that the human body must tolerate. All these can significantly affect the osseointegration process. Nevertheless, the rabbit model is reproducible, easy to handle, and cost-effective. The stability of the implant was not tested biomechanically, and the biomechanical characteristics of the newly formed bone were not investigated. The follow-up was limited to 6 and 12 weeks. According to the ANOVA, at 6 weeks all three groups were similar in BV/TV and trabecular thickness; however, small variability was evident, and whether this might influence the results at 12 weeks is unknown. Moreover, understanding the progression of new cancellous bone formation after 12 weeks on these functionalised HPOC surfaces can be of clinical benefit. Future studies should compare the performance of these functionalised HPOCs with standard materials used in arthroplasty (e.g. titanium).

Conclusion

Sinalised HPOC in isolation or functionalised with BMP-2 or RGD promote in vivo osteointegration. The sinalised HOPC functionalised with BMP-2 demonstrated the greatest osseointegration.

Abbreviations

micro CT	Micro-computed tomography
HPOC	High-performance oxide ceramics
BMP-2	Bone Morphogenetic Protein 2
SiOx	Silicon suboxide
TV	Total volume
BV	Bone volume
PE-CVD	Plasma-enhanced chemical vapour deposition
LCL	Lateral collateral ligament

MD	Mean difference
SE	Effect measure and standard error
ANOVA	Analysis of variance
VAR	Variance
SS	Sum of squares
HSD	Honestly Significant Difference
BIC	Bone-implant contact ratio

Acknowledgements
None

Author's contributions
Conceptualization, M.T., J.E.; investigation, H.S., S.L., M.B.; project administration, B.R.; supervision, F.H.; writing – original draft, F.M. and H.S. All authors have read and agreed to the published version of the manuscript.

Funding
This research was founded by the German Federal Ministry of Education and Research (Bundesministerium für Bildung und Forschung, BMBF) as part of the Validation of the Technological and Social Innovation Potential of Scientific Research (Validierung des Technologischen und Gesellschaftlichen Innovationspotenzials wissenschaftlicher Forschung) Funding (FZ: 03V0349).

Data availability
The data presented in this study are available on request from the corresponding author.

Declarations

Ethics approval and consent to participate
This study was conducted according to the Animal Welfare Act of the Federal Republic of Germany. This study was approved by the Federal Office for Nature, Environment and Consumer Protection (Landesamt für Natur, Umwelt und Verbraucherschutz, LANU) of North Rhine-Westphalia, Federal Republic of Germany (Approval ID: 84-02.04.2016.A434).

Consent for publication
Not applicable.

Competing interests
The authors declare no competing interests.

Author details
[1]Department of Orthopaedic, Trauma, and Reconstructive Surgery, RWTH University Hospital, Pauwelsstraße 30, 52074 Aachen, Germany. [2]Department of Orthopaedic and Trauma Surgery, Academic Hospital of Bolzano (SABES-ASDAA), 39100 Bolzano, Italy. [3]Department of Life Sciences, Health, and Health Professions, Link Campus University, Rome, Italy. [4]Department of Orthopaedic and Trauma Surgery, University Hospital of Erlangen, 91054 Erlangen, Germany. [5]Department of Trauma and Orthopaedic Surgery, Faculty of Medicine and Psychology, University La Sapienza, 00185 Rome, Italy. [6]Faculty of Medicine, School of Pharmacy and Bioengineering, Keele University, ST4 7QB Stoke On Trent, England. [7]Queen Mary University of London, Barts and the London School of Medicine and Dentistry, Mile End Hospital, 275 Bancroft Road, E1 4DG London, England. [8]Ortho-Centrum Aachen (OCA), Aachen, Germany. [9]Department of Orthopaedic Surgery, Klinikum Wels-Grieskirchen, 4600 Wels, Austria.

Received: 30 October 2023 Accepted: 13 July 2024
Published online: 18 July 2024

References

1. Grimberg A, Jansson VWD, Lützner J, Melsheimer O, Morlock M, Steinbrück A (2020) Endoprothesenregister Deutschland, Jahresbericht 2020.
2. Matar HE, Platt SR, Board TN, Porter ML. Overview of randomized controlled trials in primary total hip arthroplasty (34,020 patients): what have we learnt? J Am Acad Orthop Surg Glob Res Rev. 2020;4(8):e2000120. https://doi.org/10.5435/JAAOSGlobal-D-20-00120.
3. Mell SP, Wimmer MA, Jacobs JJ, Lundberg HJ. Optimal surgical component alignment minimizes TKR wear-an in silico study with nine alignment parameters. J Mech Behav Biomed Mater. 2022;125:104939. https://doi.org/10.1016/j.jmbbm.2021.104939.
4. Leskinen J, Eskelinen A, Huhtala H, Paavolainen P, Remes V. The incidence of knee arthroplasty for primary osteoarthritis grows rapidly among baby boomers: a population-based study in Finland. Arthritis Rheum. 2012;64(2):423–8. https://doi.org/10.1002/art.33367.
5. Oonishi H, Ueno M, Kim SC, Oonishi H, Iwamoto M, Kyomoto M. Ceramic versus cobalt-chrome femoral components; wear of polyethylene insert in total knee prosthesis. J Arthroplasty. 2009;24(3):374–82. https://doi.org/10.1016/j.arth.2007.10.021.
6. Trieb K. A novel ceramic tibial component is as safe as its metal counterpart. Biomed Tech (Berl). 2018;63(3):327–32. https://doi.org/10.1515/bmt-2016-0231.
7. Solarino G, Piconi C, De Santis V, Piazzolla A, Moretti B. Ceramic total knee arthroplasty: ready to go? Joints. 2017;5(4):224–8. https://doi.org/10.1055/s-0037-1607428.
8. Catauro M, Papale F, Bollino F. Coatings of titanium substrates with xCaO.(1–x)SiO2 sol-gel materials: characterization, bioactivity and biocompatibility evaluation. Mater Sci Eng C Mater Biol Appl. 2016;58:846–51. https://doi.org/10.1016/j.msec.2015.09.033.
9. Moritz N, Rossi S, Vedel E, Tirri T, Ylanen H, Aro H, Narhi T. Implants coated with bioactive glass by CO_2-laser, an in vivo study. J Mater Sci Mater Med. 2004;15(7):795–802. https://doi.org/10.1023/b:jmsm.0000032820.50983.c1.
10. Taniguchi A, Tanaka Y. An alumina ceramic total talar prosthesis for avascular necrosis of the talus. Foot Ankle Clin. 2019;24(1):163–71. https://doi.org/10.1016/j.fcl.2018.10.004.
11. Pobloth AM, Mersiowsky MJ, Kliemt L, Schell H, Dienelt A, Pfitzner BM, Burgkart R, Detsch R, Wulsten D, Boccaccini AR, Duda GN. Bioactive coating of zirconia toughened alumina ceramic implants improves cancellous osseointegration. Sci Rep. 2019;9(1):16692. https://doi.org/10.1038/s41598-019-53094-5.
12. Migliorini F, Eschweiler J, Maffulli N, Hildebrand F, Schenker H. Functionalised high-performance oxide ceramics with bone morphogenic protein 2 (BMP-2) induced ossification: an in vivo study. Life (Basel). 2022. https://doi.org/10.3390/life12060866.
13. Migliorini F, Schenker H, Maffulli N, Hildebrand F, Eschweiler J. Histomorphometry of ossification in functionalised ceramics with tripeptide Arg-Gly-Asp (RGD): an in vivo study. Life (Basel). 2022. https://doi.org/10.3390/life12050761.
14. Migliorini F, Schenker H, Betsch M, Maffulli N, Tingart M, Hildebrand F, Lecouturier S, Rath B, Eschweiler J. Silica coated high performance oxide ceramics promote greater ossification than titanium implants: an in vivo study. J Orthop Surg Res. 2023;18(1):31. https://doi.org/10.1186/s13018-022-03494-7.
15. Boke F, Giner I, Keller A, Grundmeier G, Fischer H. Plasma-enhanced chemical vapor deposition (PE-CVD) yields better hydrolytical stability of biocompatible SiOx thin films on implant alumina ceramics compared to rapid thermal evaporation physical vapor deposition (PVD). ACS Appl Mater Interfaces. 2016;8(28):17805–16. https://doi.org/10.1021/acsami.6b04421.
16. Lauria I, Kramer M, Schroder T, Kant S, Hausmann A, Boke F, Leube R, Telle R, Fischer H. Inkjet printed periodical micropatterns made of inert alumina ceramics induce contact guidance and stimulate osteogenic differentiation of mesenchymal stromal cells. Acta Biomater. 2016;44:85–96. https://doi.org/10.1016/j.actbio.2016.08.004.
17. Migliorini F, Marsilio E, Oliva F, Eschweiler J, Hildebrand F, Maffulli N. Chondral injuries in patients with recurrent patellar dislocation: a systematic review. J Orthop Surg Res. 2022;17(1):63. https://doi.org/10.1186/s13018-022-02911-1.
18. Boke F, Labude N, Lauria I, Ernst S, Muller-Newen G, Neuss S, Fischer H. Biological activation of bioinert medical high-performance oxide ceramics by hydrolytically stable immobilization of c(RGDyK) and BMP-2. ACS Appl Mater Interfaces. 2018;10(45):38669–80. https://doi.org/10.1021/acsami.8b08900.
19. Vasudev MC, Anderson KD, Bunning TJ, Tsukruk VV, Naik RR. Exploration of plasma-enhanced chemical vapor deposition as a method for thin-film

fabrication with biological applications. ACS Appl Mater Interfaces. 2013;5(10):3983–94. https://doi.org/10.1021/am302989x.
20. Li Y, Ren J, Wang B, Lu W, Wang H, Hou W. Development of biobased multilayer films with improved compatibility between polylactic acid-chitosan as a function of transition coating of SiOx. Int J Biol Macromol. 2020;165(Pt A):1258–63. https://doi.org/10.1016/j.ijbiomac.2020.10.001.
21. Kim J, Sung GY, Park M. Efficient portable urea biosensor based on urease immobilized membrane for monitoring of physiological fluids. Biomedicines. 2020. https://doi.org/10.3390/biomedicines8120596.
22. Si YJ, Ren QH, Bi L. miR-135b-5p regulates human mesenchymal stem cell osteogenic differentiation by facilitating the Hippo signaling pathway. Int J Clin Exp Pathol. 2017;10(7):7767–75.
23. Walker JM. The bicinchoninic acid (BCA) assay for protein quantitation. Methods Mol Biol. 1994;32:5–8. https://doi.org/10.1385/0-89603-268-X:5.
24. Le X, Poinern GE, Ali N, Berry CM, Fawcett D. Engineering a biocompatible scaffold with either micrometre or nanometre scale surface topography for promoting protein adsorption and cellular response. Int J Biomater. 2013;2013:782549. https://doi.org/10.1155/2013/782549.
25. McNamara LE, Burchmore R, Riehle MO, Herzyk P, Biggs MJ, Wilkinson CD, Curtis AS, Dalby MJ. The role of microtopography in cellular mechanotransduction. Biomaterials. 2012;33(10):2835–47. https://doi.org/10.1016/j.biomaterials.2011.11.047.
26. Jin S, Xia X, Huang J, Yuan C, Zuo Y, Li Y, Li J. Recent advances in PLGA-based biomaterials for bone tissue regeneration. Acta Biomater. 2021;127:56–79. https://doi.org/10.1016/j.actbio.2021.03.067.
27. Kido HW, Ribeiro DA, de Oliveira P, Parizotto NA, Camilo CC, Fortulan CA, Marcantonio E Jr, da Silva VH, Renno AC. Biocompatibility of a porous alumina ceramic scaffold coated with hydroxyapatite and bioglass. J Biomed Mater Res A. 2014;102(7):2072–8. https://doi.org/10.1002/jbm.a.34877.
28. Mohammadi H, Sepantafar M. Ion-doped silicate bioceramic coating of Ti-based implant. Iran Biomed J. 2016;20(4):189–200. https://doi.org/10.7508/ibj.2016.04.002.
29. Herberg S, Susin C, Pelaez M, Howie RN, Moreno de Freitas R, Lee J, Cray JJ Jr, Johnson MH, Elsalanty ME, Hamrick MW, Isales CM, Wikesjo UM, Hill WD. Low-dose bone morphogenetic protein-2/stromal cell-derived factor-1beta cotherapy induces bone regeneration in critical-size rat calvarial defects. Tissue Eng Part A. 2014;20(9–10):1444–53. https://doi.org/10.1089/ten.TEA.2013.0442.
30. Cha M, Jin YZ, Park JW, Lee KM, Han SH, Choi BS, Lee JH. Three-dimensional printed polylactic acid scaffold integrated with BMP-2 laden hydrogel for precise bone regeneration. Biomater Res. 2021;25(1):35. https://doi.org/10.1186/s40824-021-00233-7.
31. Migliorini F, Pilone M, Eschweiler J, Marsilio E, Hildebrand F, Maffulli N. High rates of damage to the medial patellofemoral ligament, lateral trochlea, and patellar crest after acute patellar dislocation: magnetic resonance imaging analysis. Arthroscopy. 2022;38(8):2472–9. https://doi.org/10.1016/j.arthro.2022.01.044.
32. Pobloth AM, Duda GN, Giesecke MT, Dienelt A, Schwabe P. High-dose recombinant human bone morphogenetic protein-2 impacts histological and biomechanical properties of a cervical spine fusion segment: results from a sheep model. J Tissue Eng Regen Med. 2017;11(5):1514–23. https://doi.org/10.1002/term.2049.
33. Hunziker EB, Jovanovic J, Horner A, Keel MJ, Lippuner K, Shintani N. Optimisation of BMP-2 dosage for the osseointegration of porous titanium implants in an ovine model. Eur Cell Mater. 2016;32:241–56. https://doi.org/10.22203/eCM.v032a16.
34. Fraioli R, Neubauer S, Rechenmacher F, Bosch BM, Dashnyam K, Kim JH, Perez RA, Kim HW, Gil FJ, Ginebra MP, Manero JM, Kessler H, Mas-Moruno C. Control of stem cell response and bone growth on biomaterials by fully non-peptidic integrin selective ligands. Biomater Sci. 2019;7(4):1281–5. https://doi.org/10.1039/c8bm01466c.
35. Hynes RO. Integrins: bidirectional, allosteric signaling machines. Cell. 2002;110(6):673–87. https://doi.org/10.1016/s0092-8674(02)00971-6.
36. Fraioli R, Dashnyam K, Kim JH, Perez RA, Kim HW, Gil J, Ginebra MP, Manero JM, Mas-Moruno C. Surface guidance of stem cell behavior: Chemically tailored co-presentation of integrin-binding peptides stimulates osteogenic differentiation in vitro and bone formation in vivo. Acta Biomater. 2016;43:269–81. https://doi.org/10.1016/j.actbio.2016.07.049.
37. Rappe KS, Ortiz-Hernandez M, Punset M, Molmeneu M, Barba A, Mas-Moruno C, Guillem-Marti J, Caparros C, Ruperez E, Calero J, Manzanares MC, Gil J, Franch J. On-growth and in-growth osseointegration enhancement in PM porous Ti-scaffolds by two different bioactivation strategies: alkali thermochemical treatment and RGD peptide coating. Int J Mol Sci. 2022. https://doi.org/10.3390/ijms23031750.
38. Freeman MA, Plante-Bordeneuve P. Early migration and late aseptic failure of proximal femoral prostheses. J Bone Joint Surg Br. 1994;76(3):432–8.
39. Robertsson O, Ranstam J, Sundberg M, A WD, Lidgren L,. The Swedish knee arthroplasty register: a review. Bone Joint Res. 2014;3(7):217–22. https://doi.org/10.1302/2046-3758.37.2000289.
40. Reimeringer M, Nuno N. The influence of contact ratio and its location on the primary stability of cementless total hip arthroplasty: a finite element analysis. J Biomech. 2016;49(7):1064–70. https://doi.org/10.1016/j.jbiomech.2016.02.031.
41. Viceconti M, Pancanti A, Varini E, Traina F, Cristofolini L. On the biomechanical stability of cementless straight conical hip stems. Proc Inst Mech Eng H. 2006;220(3):473–80. https://doi.org/10.1243/09544119H06904.
42. Cobo-Vazquez C, Reininger D, Molinero-Mourelle P, Gonzalez-Serrano J, Guisado-Moya B, Lopez-Quiles J. Effect of the lack of primary stability in the survival of dental implants. J Clin Exp Dent. 2018;10(1):e14–9. https://doi.org/10.4317/jced.54441.
43. Overmann AL, Aparicio C, Richards JT, Mutreja I, Fischer NG, Wade SM, Potter BK, Davis TA, Bechtold JE, Forsberg JA, Dey D. Orthopaedic osseointegration: implantology and future directions. J Orthop Res. 2020;38(7):1445–54. https://doi.org/10.1002/jor.24576.
44. Mavrogenis AF, Dimitriou R, Parvizi J, Babis GC. Biology of implant osseointegration. J Musculoskelet Neuronal Interact. 2009;9(2):61–71.
45. Heriveaux Y, Le Cann S, Fraulob M, Vennat E, Nguyen VH, Haiat G. Mechanical micromodeling of stress-shielding at the bone-implant interphase under shear loading. Med Biol Eng Comput. 2022;60(11):3281–93. https://doi.org/10.1007/s11517-022-02657-2.
46. Pijls BG, Valstar ER, Nouta KA, Plevier JW, Fiocco M, Middeldorp S, Nelissen RG. Early migration of tibial components is associated with late revision: a systematic review and meta-analysis of 21,000 knee arthroplasties. Acta Orthop. 2012;83(6):614–24. https://doi.org/10.3109/17453674.2012.747052.
47. Streit MR, Haeussler D, Bruckner T, Proctor T, Innmann MM, Merle C, Gotterbarm T, Weiss S. Early migration predicts aseptic loosening of cementless femoral stems: a long-term study. Clin Orthop Relat Res. 2016;474(7):1697–706. https://doi.org/10.1007/s11999-016-4857-5.

Publisher's Note